Check for updates

ORIGINAL ARTICLE

Assessing cell chimerism in an acute graft-versus-host disease model established in TLR4 knockout mice

Evaluación del quimerismo celular en un modelo de enfermedad aguda de injerto contra huésped establecido en ratones knockout para TLR4

*Yi Zhao[1], Xi Huang[1], Yujie Zhang[1], Donghua He[1], Jingsong He[1], Enfan Zhang[1], Miao Chen[2], Qiuyan Liu[2], Jing Chen[1], and Zhen Cai[1]**

[1]Department of Hematology, Bone Marrow Transplantation Center, The First Affiliated Hospital, School of Medicine, Zhejiang University, Hangzhou; [2]National Key Laboratory of Medical Immunology and Institute of Immunology, Second Military Medical University, Shanghai. China

Abstract

Background: *Graft-versus-host disease (GVHD) is a major complication after allogeneic hematopoietic stem cell transplantation.* **Objective:** *To elucidate the role of Toll-like receptor 4 (TLR4), the major receptor for bacterial lipopolysaccharide, in the development of GVHD, we constructed a GVHD model in TLR4 knockout (TLR4$^{-/-}$) mice and monitored the cell chimerism.* **Methods:** *In this study, we used polymerase chain reaction to identify whether TLR4 knockout (TLR4$^{-/-}$) mice were established. Before transplantation, we pretreated mice with irradiation so as to obtain an appropriate irradiation dose. Flow cytometry was applied to measure the chimerism status, the distributions of antigen-presenting cells (APCs), and T-cells in TLR4$^{+/+}$ and TLR4$^{-/-}$ recipient mice.* **Results:** *The general condition of TLR4$^{-/-}$ recipients was better than that of TLR4$^{+/+}$ recipients, and the TLR4$^{-/-}$ recipient mice showed less severe GVHD manifestations than the TLR4$^{+/+}$ recipient mice. Most of the APCs and T-cells in the host mouse spleen were derived from donor cells, and CD4^{+} T-cells, including memory T-cells, were in the majority in host mice.* **Conclusion:** *In general, our data show that TLR4 deletion attenuated GVHD development, which suggests that TLR4 could be used as a novel target and therapeutic paradigm in GVHD therapies.*

Keywords: *Acute graft-versus-host disease. Toll-like receptors 4. Cell chimerism. Mice model. Transplantation.*

Resumen

Antecedentes: *La enfermedad de injerto contra huésped (EICH) es una complicación importante después del trasplante alogénico de células madre hematopoyéticas.* **Objetivo:** *Para dilucidar el papel de TLR4, el principal receptor de LPS bacteriano, en el desarrollo de GVHD, construimos un modelo de GVHD en ratones knockout para TLR4 (TLR4-/-) y monitoreamos el quimerismo celular.* **Métodos:** *En este estudio, usamos PCR para identificar si se establecieron ratones knockout para TLR4 (TLR4-/-). Antes del trasplante, pretratamos a los ratones con irradiación para obtener la dosis de irradiación adecuada. Se aplicó citometría de flujo para medir el estado de quimerismo, las distribuciones de APC y células T en ratones receptores TLR4+/+ y TLR4-/-.* **Resultados:** *El estado general de los receptores de TLR4-/- fue mejor que el de los receptores de TLR4+/+, y los ratones receptores de TLR4-/- mostraron manifestaciones de GVHD menos graves que los ratones receptores de TLR4+/+. La mayoría de las APC y las células T en el bazo del ratón huésped se derivaron de las células del donante, y las células T CD4+, incluidas las células T de memoria, se encontraban en su mayoría en los ratones huéspedes.* **Conclusión:** *En general, nuestros datos muestran que la eliminación de TLR4 atenuó el desarrollo de GVHD, lo que sugiere que TLR4 podría usarse como un nuevo objetivo y paradigma terapéutico en las terapias de GVHD.*

***Palabras clave*:** *AGVHD. TLR4. Quimerismo celular. Modelo de ratones. Trasplante.*

***Correspondence:**
Zhen Cai
E-mail: caiz@zju.edu.cn

Date of reception: 16-08-2022
Date of acceptance: 29-12-2022
DOI: 10.24875/CIRUE.M22000726

Cir Cir (Eng). 2023;91(5):583-596
Contents available at PubMed
www.cirugiaycirujanos.com

2444-0507/© 2022 Academia Mexicana de Cirugía. Published by Permanyer. This is an open access article under the terms of the CC BY-NC-ND license (http://creativecommons.org/licenses/by-nc-nd/4.0/).

Introduction

Acute graft-versus-host disease (aGVHD) is the most common complication of allogeneic bone marrow transplantation (BMT) associated with effector T-cells that result from the recognition of host histocompatibility antigens (both major and minor) by donor T-cells[1,2]. Despite the use of preventive measures, aGVHD affects 30-70% of recipients and remains a major life-threatening problem in allogeneic transplantation[3,4]. Thus, there is an urgent need to reveal the mechanism underlying GVHD and to develop the long-term post-transplant outcomes and quality of life of recipients.

The innate immune response plays a major role in the development of GVHD. Gram-negative bacteria and their cell wall component lipopolysaccharide (LPS) activate innate immune response receptors, including Toll-like receptors (TLRs), and cause a cascade of cytokine release that is closely related to the development of GVHD[5]. A study of 237 patients indicated that mutations in TLR4 reduce the risk of aGVHD and may increase the risk of Gram-negative bacteremia in allogeneic bone marrow transplant recipients[6]. In addition, heparan sulfate can activate TLR4 and promote aGVHD, and serum heparan sulfate levels are positively correlated with the severity of GVHD after allogeneic stem cell transplantation[7].

Most of the current knowledge underlying the understanding of the pathophysiology of GVHD, as well as the development of new treatment regimens, derives from studies with animal models[8]. The use of a mouse model of allogeneic BMT is an ideal method to explore the pathogenesis of GVHD since humans and mice have similar manifestations of GVHD after transplantation. MHC mismatches between donor and recipient mice can lead to severe GVHD, which can be observed experimentally. Using a mouse model to study, the role of TLR4 in GVHD will undoubtedly be a good choice.

BALB/c and C57BL/6 mice are purebred congenic mouse strains with different major and minor histocompatibility antigens (MHC-I and MHC-II) and are available for graft rejection studies. Allogeneic BMT models using C57BL/6 and BALB/c mice have been established by different laboratories worldwide, but BALB/c and TLR4 knockout mouse models of GVHD have rarely been reported. Due to different GVHD conditions in mouse models resulting from different mouse origins, rearing conditions, and radioactive sources, it is necessary to establish a TLR4 knockout mouse model suitable for local experimental conditions. Our laboratory established a TLR4 knockout ($TLR4^{-/-}$) mouse GVHD model for allogeneic BMT between $TLR4^{+/+}$ and BALB/c mice or $TLR4^{-/-}$ and BALB/c mice[9]. Among these mice, BALB/c mice have strong productivity and a long idiophase but are sensitive to carcinogenic factors and radiation. TLR4 knockout ($TLR4^{-/-}$) mice are on the same background as C57BL/6 mice ($TLR4^{+/+}$). We found that TLR4 inactivation attenuated GVHD, but the relationship between TLR4 and the development of GVHD is still unknown.

BMT can create a permanently chimeric individual containing original diseased cells and newly transplanted healthy cells that convey a therapeutic effect in the form of a healthy gene. The level of chimerism can effectively evaluate the occurrence of moderate to severe aGVHD after transplantation[10]. Monitoring variations in cell chimerism early after transplantation help to identify patients at risk for graft rejection or grade II-IV aGVHD[11,12]. In this study, we explored the pathogenesis, development, and especially cell chimerism of GVHD and further observed changes in immune-related cells during transplantation in the absence or presence of TLR4 as well as possible mechanisms using TLR4 knockout mice. We determined the success of transplantation by assessing symptoms, signs, and the chimerism state after transplantation. This model helped us to investigate the molecular mechanism underlying GVHD in depth and laid the experimental basis for finding new targets for controlling GVHD.

Materials and methods

Reagents and antibodies

RPMI 1640 medium and fetal bovine serum were obtained from PAA Laboratories (Linz, Austria). Fluorescein-conjugated monoclonal antibodies (mAbs), including isotype control mAbs and mAbs against H-$2K^b$, H-$2K^d$, CD4, CD8, CD11c, CD62L, and CD44, were purchased from BD Pharmingen, BioLegend, or eBioscience Laboratories (San Diego, CA). A 2% acetic acid solution was prepared as a white blood cell (WBC) diluent. FASTLysing™ Solution was obtained from Immuno Probe (Sigma-Aldrich Co. LLC, St. Louis, MO, USA).

Mice

BALB/c (H-$2k^d$) and C57BL/6 (H-$2k^b$) mice as well as wild-type (WT) control mice were obtained from

Joint Ventures Sipper BK Experimental Animal Co. (Shanghai, China). TLR4 knockout mice ($TLR4^{-/-}$) on the same background as C57BL/6 mice ($TLR4^{+/+}$) were obtained from our breeding colony and were originally provided by Shizuo Akira (Osaka University, Japan)[13]. All mice at 8-12 weeks old (20-25 g body weight) were housed under pathogen-free conditions at constant temperature and humidity. Animal experiments were performed in accordance with the National Institutes of Health Guide for the Care and Use of Laboratory Animals with the approval of the Scientific Investigation Board of the Second Military Medical University, Shanghai, China.

Polymerase chain reaction (PCR)

DNA was extracted from tail samples from mice prepared for transplantation using the Puregene DNA Isolation Kit (according to the directions provided by the company, Shanghai Generay Biotech Co., Ltd.). An PCR kit was obtained from TaKaRa (Premix Ex Taq Ver2.0). PCR products were electrophoresed on a 1% agarose gel. PCR primers were synthesized by Sangon Biotech Co., Ltd. (Shanghai). The primer sequences for TLR4 were F1: 5'-tgt tgc cct tca gtc aca gag act ctg-3', F2: 5'-cgt gta aac cag cca ggt ttt gaa ggc-3', and F3: 5'-tgt tgg gtc gtt tgt tcg gat ccg tcg-3'. TLR4 mutation sequences were tested with F1 and F3, while WT sequences were tested with F1 and F2.

Bone marrow cell isolation

Cells from the spleen and bilateral femurs and tibia of euthanized mice were collected in a laminar flow cabinet. The collected spleens were cut with eye scissors and ground in fresh RPMI 1640 medium. The spleen suspension was passed through 40-μm nylon mesh, and the filtered cells were collected and used as the splenic mononuclear cell suspension. The collected femurs and tibia were cut, and the bone marrow cells were flushed out with an injector. The cells were collected, passed through 40-μm nylon mesh, and resuspended in RPMI 1640 medium to acquire a mononuclear cell suspension. The bone marrow cells and splenocytes were mixed together at the same volume, with the bone marrow cells at a concentration of 2.5×10^7/mL and the splenocytes at a concentration of 5×10^7/mL. Live cells were counted with trypan blue staining, and cell viability was above 95%.

Selection of irradiation dose

Before transplantation, we pretreated mice with irradiation. Mice from different strains or different units of the animal center had different stress tolerances to radiation dose. Referring to domestic and foreign reports[14-18], we performed a preliminary study with TLR4-deficient mice with a single dose of 9-10 Gy and showed that the mice died of radiation sickness within 7 days with severe swelling of the gastrointestinal mucosa and substantial development of yellow hydrops. This explains why the radiation dose reported is an overdose and not suitable for our experiment. We, further, identified several exposure doses for comparison studies. We used a ^{60}Co γ-ray source in our experiment and set the doses at 6.5, 7, 7.5, 8, 8.5, 9, 10, and 11 Gy with a dose rate of 0.8 Gy/min or 1.6 Gy/min. $TLR4^{+/+}$ and $TLR4^{-/-}$ mice received one or two rounds of irradiation.

BMT

Recipient mice were housed under pathogen-free conditions at constant temperature and humidity for 1 week before transplantation. Gentamicin (320 mg/L) was added into the drinking water beginning 7 days before transplantation, and gentamicin-containing water was administered until 4 weeks after BMT when antibiotic treatments were stopped. Recipient C57BL/6 mice underwent lethal total body irradiation (TBI) using a ^{60}Co irradiator. All irradiation procedures were performed as a single dose. Four hours later, the recipient mice were injected with 0.4 mL of mixed bone marrow cell and splenocyte suspension through the tail vein. Every mouse received approximately 1.0×10^7 bone marrow cells and 2.0×10^7 splenocytes in total. The simple radiation group was injected with only 0.4 mL of PBS solution through the tail vein, while the isograft group was injected with 0.4 mL of syngeneic bone marrow cells and splenocytes.

Peripheral blood leukocyte counts of mice

WBCs were counted every 3 days within the 1st month after transplantation and every 7 days for the next month. Twenty microliters of blood were obtained with a pipette after cutting the tails of randomly selected mice. Then, each tail sample was mixed with 380 μL of 2% acetic acid, and Tris-NH_4Cl was added. Once the cloudy solution cleared on

standing, 20 μL of solution was transferred to a cell counter for counting the WBCs from the peripheral blood of the mice. The time when the WBC count was the lowest and the time when it was normal were observed. A WBC count > 1.0 × 10^9/L was regarded as hematopoietic reconstitution. Every group consisted of at least three mice, and the data are shown as the mean ± SD.

Flow cytometry (FCM)

Fifty microliters of peripheral blood were collected from recipient mice by retro-orbital puncture using heparin for anticoagulation. The cells were treated with FASTLysing™ Solution (BD) to lyse red blood cells and were washed twice with PBS. The percentage of chimeric cells was detected by FCM after an incubation with FITC-conjugated anti-H-2K^b and PE-conjugated anti-H-2K^d antibodies at 4°C for 15 min. Splenic mononuclear cell suspensions were incubated with FITC-conjugated anti-H-2K^b, PE-conjugated anti-H-2K^d, and PerCP-conjugated anti-CD4 antibodies or with FITC-conjugated anti-H-2K^b, PE-conjugated anti-H-2K^d, and PerCP-conjugated anti-CD11c antibodies to detect the chimerism of CD4$^+$ T-cells and antigen-presenting cells (APCs), respectively, in the spleen of recipient mice. Suspensions were incubated with FITC-conjugated anti-CD4 and PE-conjugated anti-CD8 antibodies to measure the proportions of CD4$^+$ T-cells and CD8$^+$ T-cells, respectively, in the spleen of chimeric animals by FCM. Suspensions were incubated with FITC-conjugated anti-CD62L and PE-conjugated anti-CD44 antibodies to measure the percentages of memory T-cells and naive T-cells through FCM. The cells were analyzed using FACS-Calibur and LSR II flow cytometers (BD Biosciences, San Jose, CA, USA). Data were analyzed by FlowJo (TreeStar).

Immunofluorescence and immunohistochemical analyses

The right lobe of the liver, proximal small intestine, and neck skin of mice were collected and fixed in 5% formalin. Then, 5-μm-thick paraffin-embedded sections were cut and stained with hematoxylin and eosin (HE). Histopathological changes in different organs were evaluated with light microscopy. T-cells labeled with a FITC-conjugated anti-CD4 antibody, a PE-conjugated anti-CD8 antibody, and DAPI were examined by fluorescence microscopy to detect infiltrating lymphocytes in the liver.

Assessment of GVHD in transplanted animals

As reported, clinical GVHD was assessed by a scoring system including five parameters: Weight loss, posture (hunching), activity, fur texture, and skin integrity[19]. Mice were euthanized, and the liver, spleen, lymph node, small intestine, and skin on the back of the neck were evaluated to determine the pathological grade of GVHD according to the scoring system[9,20].

Statistical analysis

Data are shown as the mean ± SD or %, and the GVHD grading analysis was assessed by Student's t-test. Survival analysis was performed by the log-rank test. SPSS16.0 for statistical analysis was applied for statistical processing. All experiments were performed in triplicate as three independent assays. $p < 0.01$ represents a significant difference, while $p < 0.05$ indicates a statistical difference.

Results

Validation of TLR4 knockout (TLR4$^{-/-}$) mice

To guarantee the reliability of our data, we verified TLR4 knockout (TLR4$^{-/-}$) mice and C57BL/6 wild-type mice. Gel electrophoresis of the PCR products indicated that compared with positive controls (lanes 10 and 11), TLR4 was successfully knockout in samples from TLR4$^{-/-}$ mice (lanes 1 to 9) (Fig. 1A), while TLR4 was positively expressed in samples from C57BL/6 wildtype mice (lanes 1 to 9) in comparison with negative controls (lanes 10 and 11) (Fig. 1B). All of these results demonstrated that the TLR4$^{-/-}$ mice we used were inbred mice, insuring high homogeneity in genetic characteristics. C57BL/6 wildtype mice provided by a company were used as TLR4$^{+/+}$ mice.

TLR4$^{-/-}$ mouse model of allogeneic BMT

We, further, identified several exposure doses for comparison studies. We used a ^{60}Co γ-ray source in our experiment and set the doses at 6.5, 7, 7.5, 8, 8.5, 9, 10, and 11 Gy with a dose rate of 0.8 Gy/min or 1.6 Gy/min. Those mice that received a single dose of 7.5-8.5 Gy at a dose rate of 0.8 Gy/min had a 30-day survival rate between 25% (3/12) and 58% (7/12).

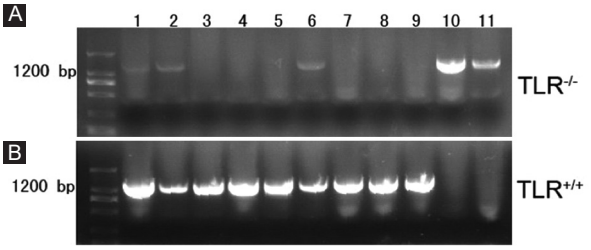

Figure 1. *Identification of TLR4 knockout (TLR4$^{-/-}$) mice. Gel electrophoresis of polymerase chain reaction (PCR) products;* **A:** *lanes 1-9 contain PCR products from TLR4$^{-/-}$ mice amplified by F1 and F3 with a size of 1,200 bp. Lanes 10 and 11 served as positive controls.* **B:** *lanes 1-9 contain PCR products from TLR4$^{+/+}$ mice amplified by F1 and F2 with a size of 1,200 bp. Lanes 10 and 11 served as negative controls.*

Furthermore, compared to the mice given a single dose, the mice that received two doses with a 3- to 4-h intervening interval had a higher maximum tolerated dose. For example, the maximum tolerated dose in C57BL/6 mice can reach 10.5 Gy with no deaths within 7 days. Referring to this study, we determined our optimal radiation dose. Recipient TLR4$^{+/+}$ and TLR4$^{-/-}$ mice received 8 Gy as single-fraction irradiation with a dose rate of 0.8 Gy/min.

To perform experiments, we grouped transplanted mice. The mice in TLR4$^{-/-}$ and TLR4$^{+/+}$ groups, which each contained fifteen mice, were injected with a suspension containing bone marrow cells and splenocytes from MHC-mismatched BALB/c donor mice (Fig. 2). The control groups contained six mice each and included a simple radiation group (mice given the same feed and pretreatment as the TLR4$^{-/-}$ group and TLR4$^{+/+}$ group mice but without transplantation, received an injection of only a PBS solution) and an isograft group (mice given the same feed and pretreatment but injected with a combination of syngeneic bone marrow cells and splenocytes). The mice in all the groups were the same age and sex. We notched the ears of the recipient mice for identification. Discrepancies in body weight were < 1 g, and the differences in mouse weights between two groups were not significantly different ($p > 0.05$) (Table 1).

Chimerism status detection in the peripheral blood of TLR4$^{-/-}$ recipient mice

To explore the time required for hematopoietic reconstitution in TLR4$^{-/-}$ mice after transplantation and the chimerism status of blood cells in recipient mice, we obtained 50 μL of peripheral blood of mice every 2 days after transplantation. FCM was used for dynamic observation of donor and recipient blood cell conversion by following the markers H-2K^b/H-2K^d. The results suggested that before transplantation, recipient mouse (C57BL/6) blood cells all expressed H-2K^b, and donor mouse (BALB/c) blood cells all expressed H-2K^d (Fig. 3A). Donor hematocytes from the donor mice could be detected in the peripheral blood of the recipient mice as early as 2 days after transplantation. The proportion of hematocytes rapidly increased over time, it reached 70% on the 10th day, was close to the original level on the 14th day, and was almost 100% on the 30th day, indicating that the donor bone marrow had implanted successfully (Fig. 3B and C).

General condition of TLR4$^{-/-}$ recipients was better than that of TLR4$^{+/+}$ recipients after transplantation

Mice were grouped as described above, and symptoms and signs of GVHD including the survival rate, body weight, and WBC count were monitored. Six mice in the simple radiation group died of bone marrow failure with WBC counts below 0.5×10^9/L. One mouse in the isograft control group died of acute radiation sickness on the 7th day, while the other five mice survived long-term and resumed normal hematopoiesis. Only two TLR4$^{+/+}$ recipient mice (13.3%) lived beyond 65 days, while four TLR4$^{-/-}$ recipient mice (26.7%) lived beyond 65 days and exhibited long-term survival (Fig. 4A). All the TLR4$^{+/+}$ and TLR4$^{-/-}$ recipient mice showed weight loss. As time progressed, the mice with severe GVHD had obvious weight loss of more than 30% and even died. The mice with mild GVHD also had decreases in weight, but to a lesser degree than that observed in the severe GVHD mice, further, their weight returned to normal during hematopoiesis recovery. The mice that survived long-term exhibited increases in weight over time. Mice that received a syngraft also had weight loss early after transplantation, with their lowest weights occurring on the 10th day, but their weights returned to normal during hematopoiesis recovery (Fig. 4B). The WBC count was significantly decreased in all mice on the 3rd day after transplantation, and agranulocytosis occurred on the 5th day. Recovery of hematogenesis could be seen 7 days after transplantation in some mice. The mice that received a syngraft showed the quickest hematopoiesis recovery and could be considered normal at 20 days. Due to GVHD, the TLR4$^{+/+}$ and

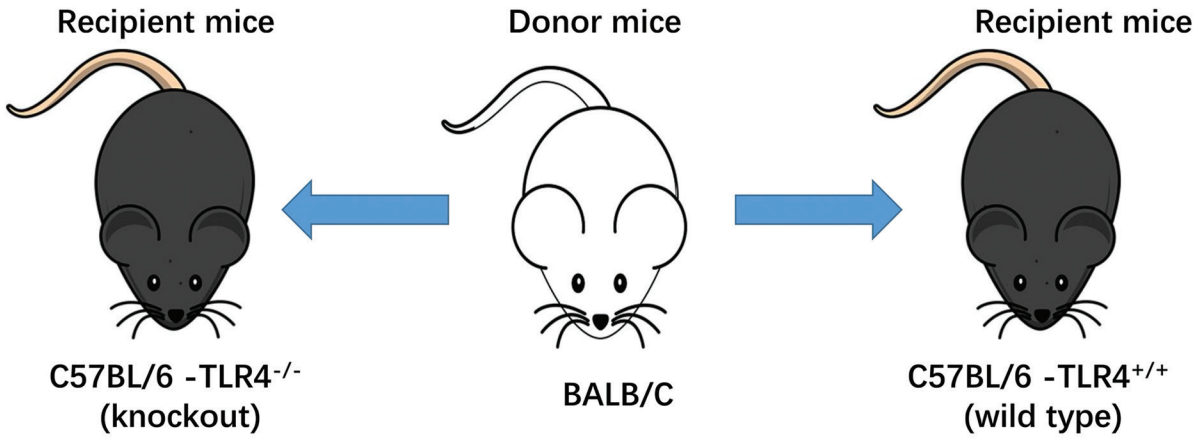

Figure 2. *Schematic for the TLR4$^{-/-}$ mouse model of allogeneic bone marrow transplantation.*

Table 1. Mouse groupings in the experiment

Groups	Donor	Recipient	Number of mice	Grafts
Simple radiation	-	C57BL/6 (TLR4$^{+/+}$ +TLR4$^{-/-}$)	6+6	-
Isograft	C57BL/6	C57BL/6 (TLR4$^{+/+}$ +TLR4$^{-/-}$)	6+6	1.0×10^7 bone marrow cells+2.0×10^7 splenocytes
TLR4$^{+/+}$	BALB/C	C57BL/6 (TLR4$^{+/+}$)	15	1.0×10^7 bone marrow cells+2.0×10^7 splenocytes
TLR4$^{-/-}$	BALB/C	C57BL/6 (TLR4$^{-/-}$)	15	1.0×10^7 bone marrow cells+2.0×10^7 splenocytes

TLR4$^{-/-}$ recipient mice showed significant hematopoiesis fluctuation. Recovery of hematogenesis could be observed at approximately 35 days in the mice that lived longer than 35 days (Fig. 4C).

Distribution of APC and T-cells in TLR4$^{+/+}$ and TLR4$^{-/-}$ mouse after transplantation

Furthermore, we investigated the absolute numbers of APCs, CD4$^+$ T-cells, and CD8$^+$ T-cells of host origin, which could increase the precision of our initial observations. The results showed in Figures 5A and B that the proportion of CD4$^+$ T-cells in the host mouse spleen had no significant difference while APCs in the host mouse spleen which derived from donor mouse was different, from 97.3% in TLR4$^{+/+}$ mice decreased to 85.6% in TLR4$^{-/-}$ mice. In addition, we explored the activation of CD4$^+$ T-cells from recipient mouse spleens both before and after transplantation. As a result, we found that the frequency of naive T-cells (CD44$^-$ CD62L$^+$) in the host mice decreased from 53% to 27%, while the proportion of memory T-cells (CD44$^+$ CD62L$^-$) increased from 27% to 37% after transplantation. We also detected the proportion of CD4$^+$ T-cells in the host mouse liver and found that memory T-cells were the major population in TLR4$^{-/-}$ mice (48%). The proportion of memory T-cells of TLR4$^{+/+}$ mice is higher than that of TLR4$^{-/-}$ mice (Fig. 5C). The proportions of T-cell subsets, including CD4$^+$ and CD8$^+$ T-cells, in the host spleen, were observed on the 30th day after transplantation. We found that the proportion of CD4$^+$ T-cells was approximately 1.5 times higher than that of CD8$^+$ T-cells (42% vs. 25%, respectively) in the TLR4$^{+/+}$ mouse while < 1.5 times in TLR4$^{-/-}$ mice (38% vs. 29%, respectively) through FCM (Fig. 5D).

In addition, we collected the right lobe of the liver of TLR4$^{-/-}$ mice on the 30th day after transplantation. The distributions of T-cell subsets, including CD4$^+$ T-cells and CD8$^+$ T-cells in the recipient mouse liver were examined by fluorescence microscopy. To directly recognize the specific site of infiltrating T-cells in the liver, we, further, performed HE staining of the same liver specimen. We concluded that both CD4$^+$ and CD8$^+$ T-cells infiltrated into the GVHD liver and that CD4$^+$ T-cells were the major cell population (Fig. 5E-G). This result is basically consistent with the results obtained by FCM.

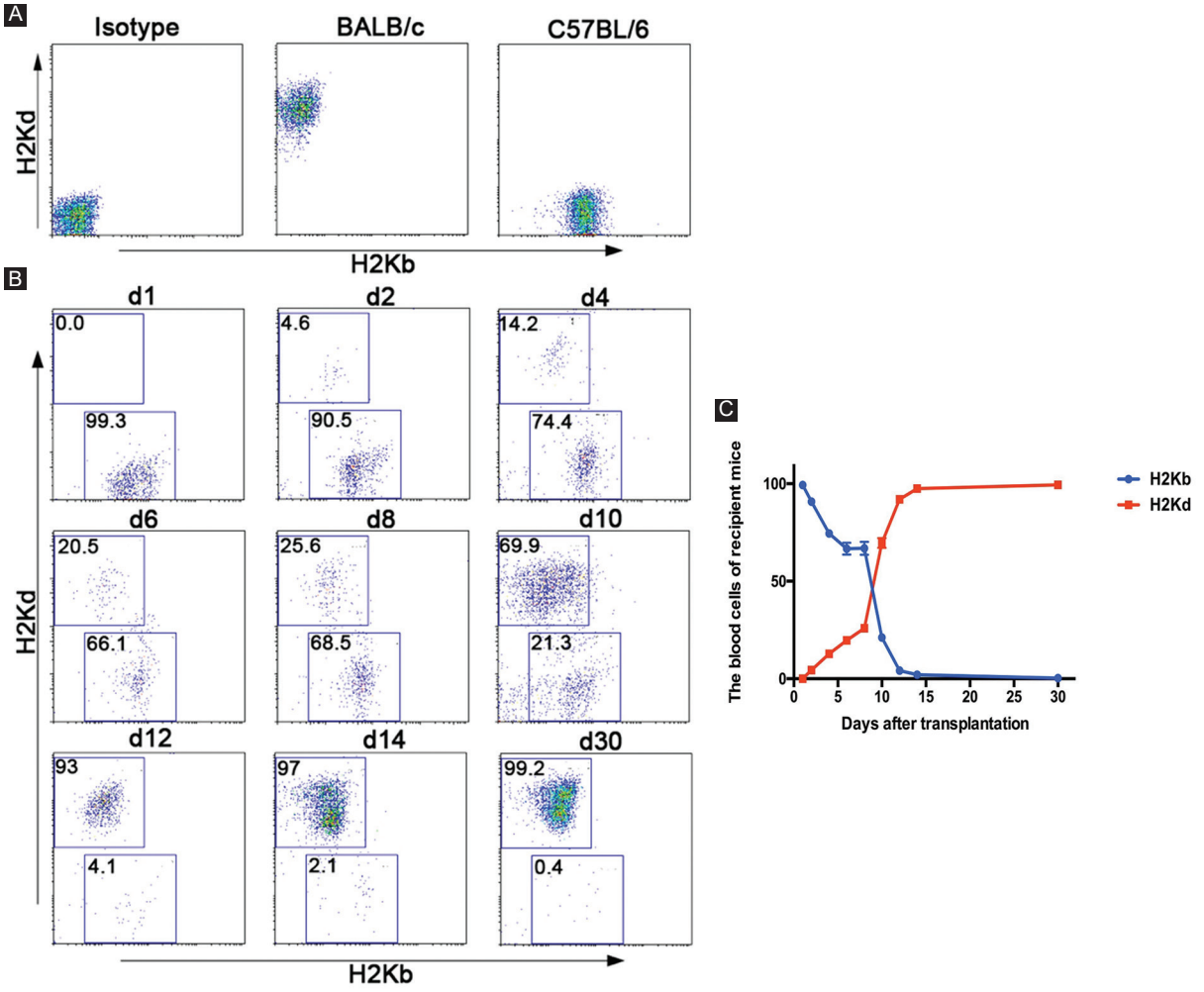

Figure 3. *Chimerism status detection in the peripheral blood of TLR4$^{-/-}$ recipient mice.* **A:** *the blood cells of recipient mice (C57BL/6-TLR4$^{-/-}$) and donor mice (BALB/c) were assessed by FCM through an incubation with FITC-conjugated anti-H-2K^{b} and PE-conjugated anti-H-2K^{d} antibodies before transplantation.* **B** and **C:** *the blood cells of recipient mice (C57BL/6-TLR4$^{-/-}$) were assessed by FCM through an incubation with FITC-conjugated anti-H-2K^{b} and PE-conjugated anti-H-2K^{d} antibodies before transplantation and on the indicated days after transplantation. The right linear graph showed the blood cells of 15 recipient mice (C57BL/6-TLR4$^{-/-}$).*

TLR4$^{-/-}$ recipient mice showed a lower degree of GVHD manifestation than TLR4$^{+/+}$ recipient mice

TLR4$^{+/+}$ and TLR4$^{-/-}$ recipient mice showed typical GVHD manifestations such as weight loss, hunching, ruffled fur texture, poor grooming, depilation, fur color fading, and decreased activity 10 days after allogeneic BMT (Fig. 6A). The TLR4$^{-/-}$ recipient mice showed lower levels of GVHD manifestation than the TLR4$^{+/+}$ recipient mice (hunching, fur color fading, and depilation) (Fig. 6B). Interestingly, we found that the TLR4$^{-/-}$ recipient mice with GVHD presented depilation, and the new fur of some long-term-surviving mice turned white (the same fur color as the donor mice) after 1 month, while the old fur remained black (the original fur color of the recipient mice). As time went on, the white fur grew more and more. Sixty days after transplantation, the mice appeared gray (Fig. 6C).

We also detected histopathological changes in GVHD. Twenty-one days after allogenic BMT, obvious discrete petechiae were observed on all the liver surfaces of TLR4$^{+/+}$ mice, and even small petechiae were observed on the surface of the spleen and intestine in one mouse. No obvious petechiae were observed in TLR4$^{-/-}$ mice (Fig. 7A). HE staining revealed that all tissues and organs of the recipient mice, especially those of the TLR4$^{+/+}$ mice, had occurrences of GVHD, while TLR4$^{-/-}$ mice have almost no GVHD symptoms as normal mice (Fig. 7B). A large number of infiltrating

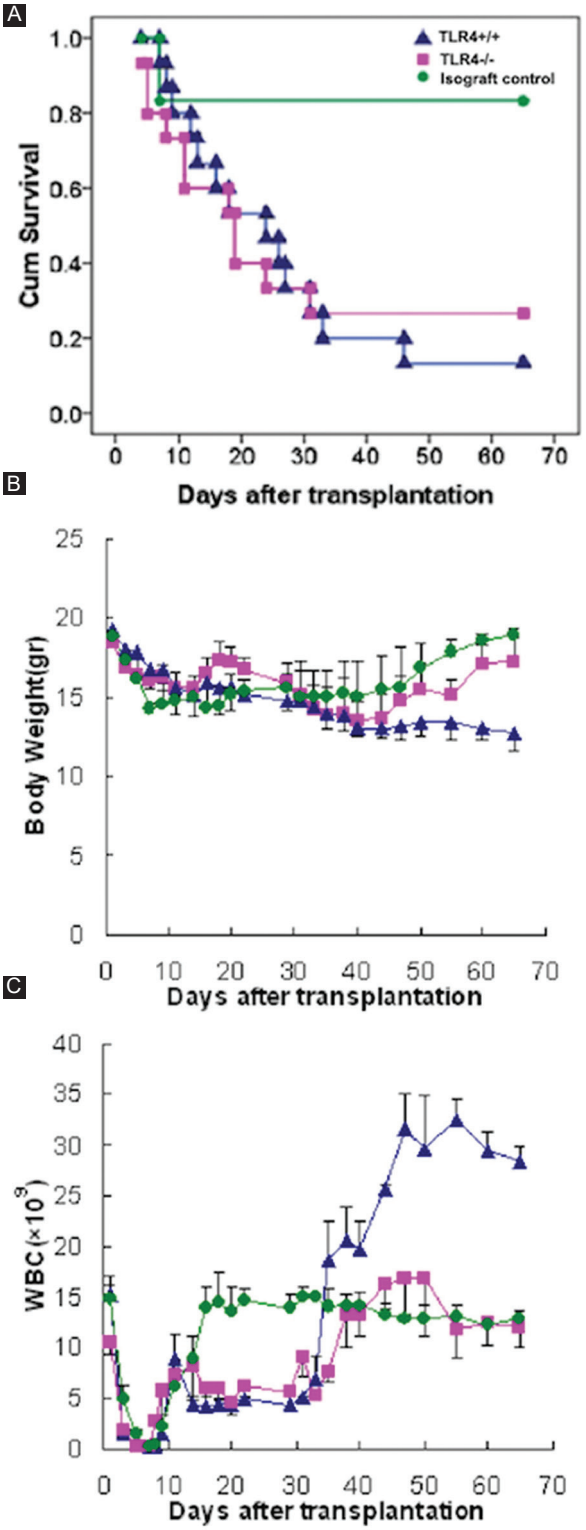

Figure 4. *Life spans, weights, and WBC counts of mice after transplantation.* **A-C:** *life spans, weights, and WBC counts were used to compare the general condition between TLR4$^{-/-}$ recipients and TLR4$^{+/+}$ recipients after transplantation. Green: Isograft control group with BALB/c recipient mice. Blue: Experimental group with TLR4$^{+/+}$ recipient mice. Pink: Experimental group with TLR4$^{-/-}$ recipient mice.*

lymphocytes, liver cell degeneration, and hepatic lobule structural damage were observed in the liver portal area. Expansion and congestion in the central vein of the portal area and hepatic blood sinus, inflammation in the bile duct area, and vascular endothelium and necrosis in biliary epithelial cells were observed. In the spleen, the structures of the red pulp and white pulp were not clear, the normal structure of the trabecula was destroyed, and the splenic corpuscle disappeared; in addition, lymphoid cell invasion, splenocyte degeneration, and necrosis were observed. In the lymph node, fibrosis could be seen along the structures of the cortex and medulla, and lymphoid follicles were not clear. The following small intestine histopathological manifestations were observed: sloughing off of the mucous membrane, necrosis of gland cells, blunting of the villus, loss of crypts, formation of slough resulting from cell debris, infiltration of inflammatory cells in the substantia propria, and formation of apoptotic bodies. A large granulomatous structure formed by a large number of inflammatory cells and lymphocyte infiltration was observed in the intestinal mucosa. In the skin, basal-layer cells were vacuolated, degenerated or necrotic, and local lymphoid cells and inflammatory cell infiltration could be seen in the subcutaneous tissue.

Discussion

GVHD is the most common complication after allogeneic BMT and contributes to multiorgan damage, immunodeficiency, and infection. There are many factors resulting in GVHD even in the case of MHC matching. TLR4 signaling related to LPS plays a critical role in the occurrence of aGVHD. Our study addressed an aGVHD mouse model with TLR4 knocked out and aimed to identify changes in cell chimerism and GVHD during the establishment of the mouse model. We propose an assumption related to monitoring a preferred level of chimerism in stem cell and gene therapies by extrapolating these findings to humans.

In this report, we needed to ensure that recipient mice were not killed by radiation sickness and that radiation sickness did not affect the observed indicators so that the GVHD model in TLR4 gene-deficient mice could be established to further study survival, body weight, and GVHD progression after allogeneic BMT. To protect recipients from radiation sickness, we

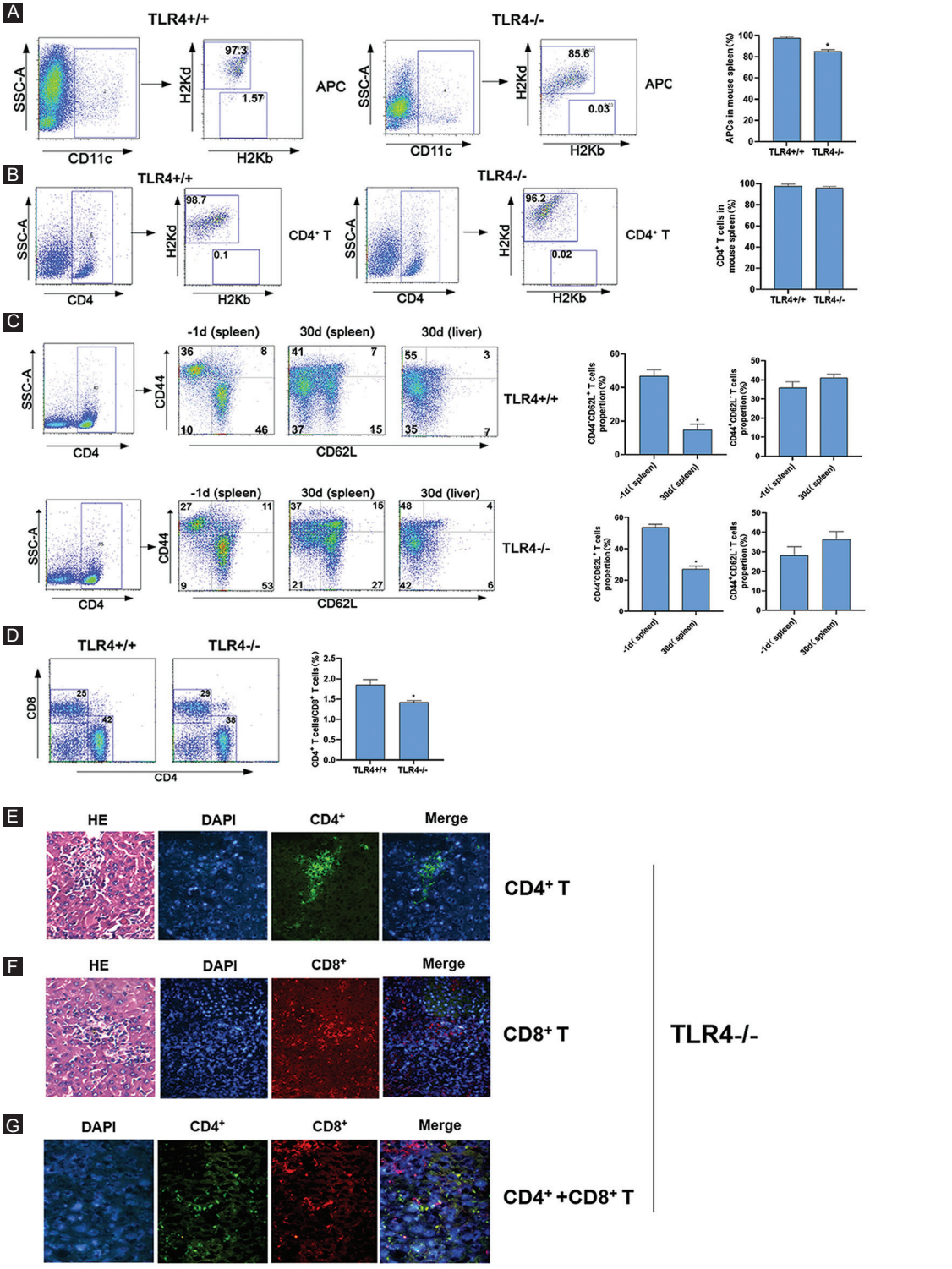

Figure 5. *Distributions of APCs and T-cells in TLR4$^{+/+}$ and TLR4$^{-/-}$ recipient mice after transplantation.* **A** and **B:** *single-cell splenocyte suspensions from recipient mice were assessed by FCM through an incubation with FITC-conjugated anti-H-2K^{b}, PE-conjugated anti-H-2K^{d} and PerCP-conjugated anti-CD11c antibodies or with FITC-conjugated anti-H-2K^{b}, PE-conjugated anti-H-2K^{d} and PerCP-conjugated anti-CD4 antibodies 30 days after transplantation.* **C:** *cell suspensions from recipient mice were assessed by FCM through an incubation with FITC-conjugated anti-CD62L and PE-conjugated anti-CD44 antibodies on the indicated days before or after transplantation.* **D:** *single-cell splenocyte suspensions from recipient mice were assessed by FCM through an incubation with FITC-conjugated anti-CD4 and PE-conjugated anti-CD8 antibodies on the 30th days after transplantation.* **E:** *immunofluorescence and HE staining analyses of invasive infiltration CD4^{+} T-cells in the liver (×200). Nuclei were stained with DAPI.* **F:** *immunofluorescence and HE staining analyses of invasive infiltration CD8^{+} T-cells in the liver (×200). Nuclei were stained with DAPI.* **G:** *immunofluorescence staining analysis of invasive CD4^{+} and CD8^{+} T-cells in the liver (×400). Nuclei were stained with DAPI. The right histograms show the relative average optical (AO) value of T-cells.*

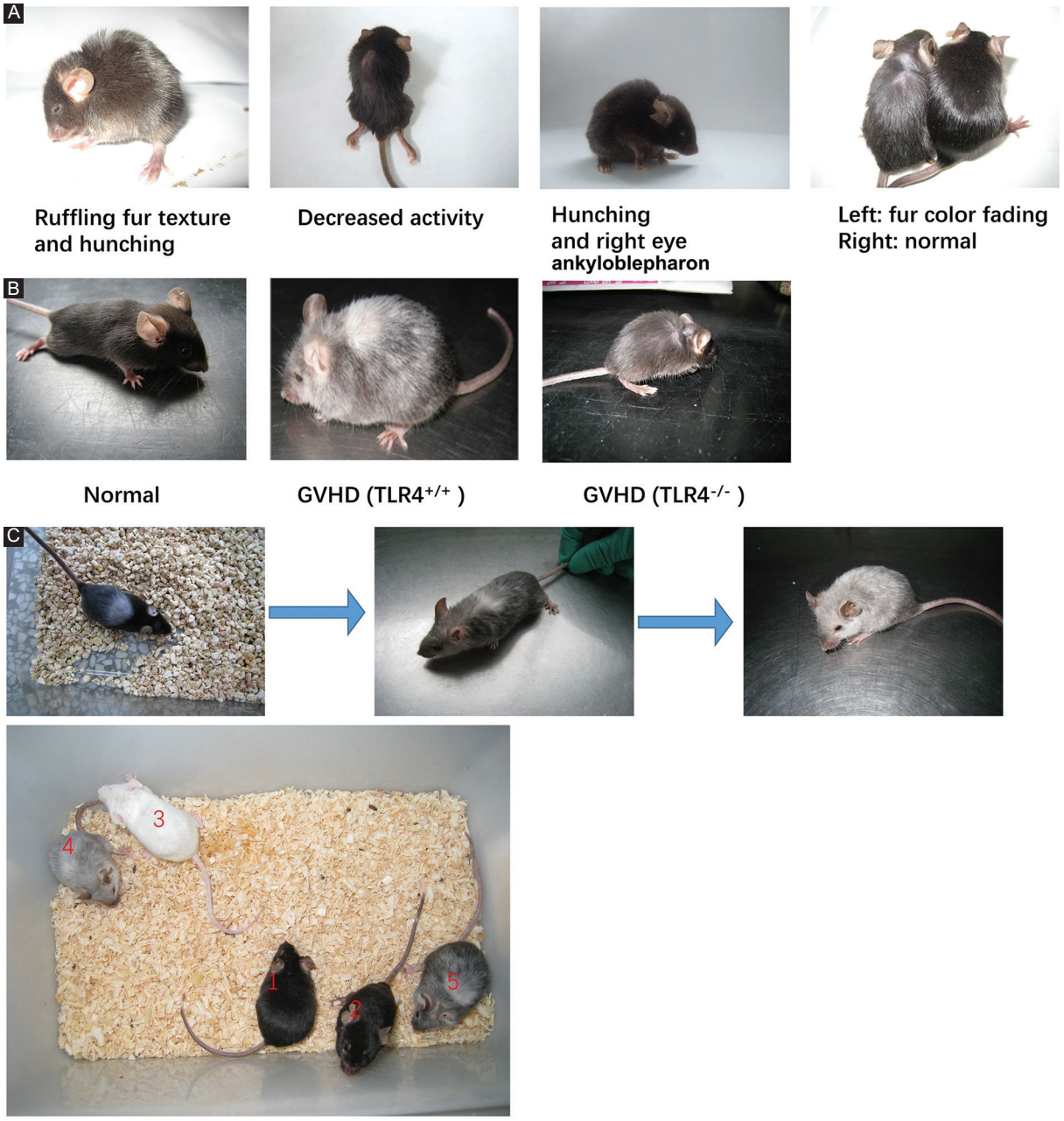

Figure 6. *Graft-versus-host disease (GVHD) occurred in mice after allogeneic bone marrow transplantation.* **A:** *GVHD manifestations in recipient mice compared with those in normal C57BL/6 mice 10 days after allogeneic bone marrow transplantation.* **B:** *GVHD manifestations of TLR4$^{-/-}$ recipient mice and TLR4$^{+/+}$ recipient mice.* **C:** *the four colors of TLR4$^{-/-}$ recipient mice, normal C57BL/6 mice and normal BALB/c mice (1 and 2 indicates normal C57BL/6 mice, 3 indicates normal BALB/c mice, 4 and 5 indicates mice after transplantation).*

chose a single-fraction TBI dose of 8.0 Gy with a dose rate of 0.8 Gy/min. Experimental data suggested that all the recipient mice showed hematopoietic reconstitution at this dose. In addition, 26.7% (4/15) lived longer than 60 days. Our data better reflect the parameters of life span, body weight, WBC counts, and other indicators. However, GVHD occurred later and to a lesser degree, which is hard to observe, in TLR4$^{-/-}$ mice than in TLR4$^{+/+}$ mice, perhaps because the decreased immunity of TLR4-deficient mice affects the GVHD response.

It has been demonstrated that GVHD can be induced only by a mixture containing splenocytes. Donor T-cells are the main effector cells in GVHD. Since we collected bone marrow cells through the elution method rather than by clinical bone marrow aspiration,

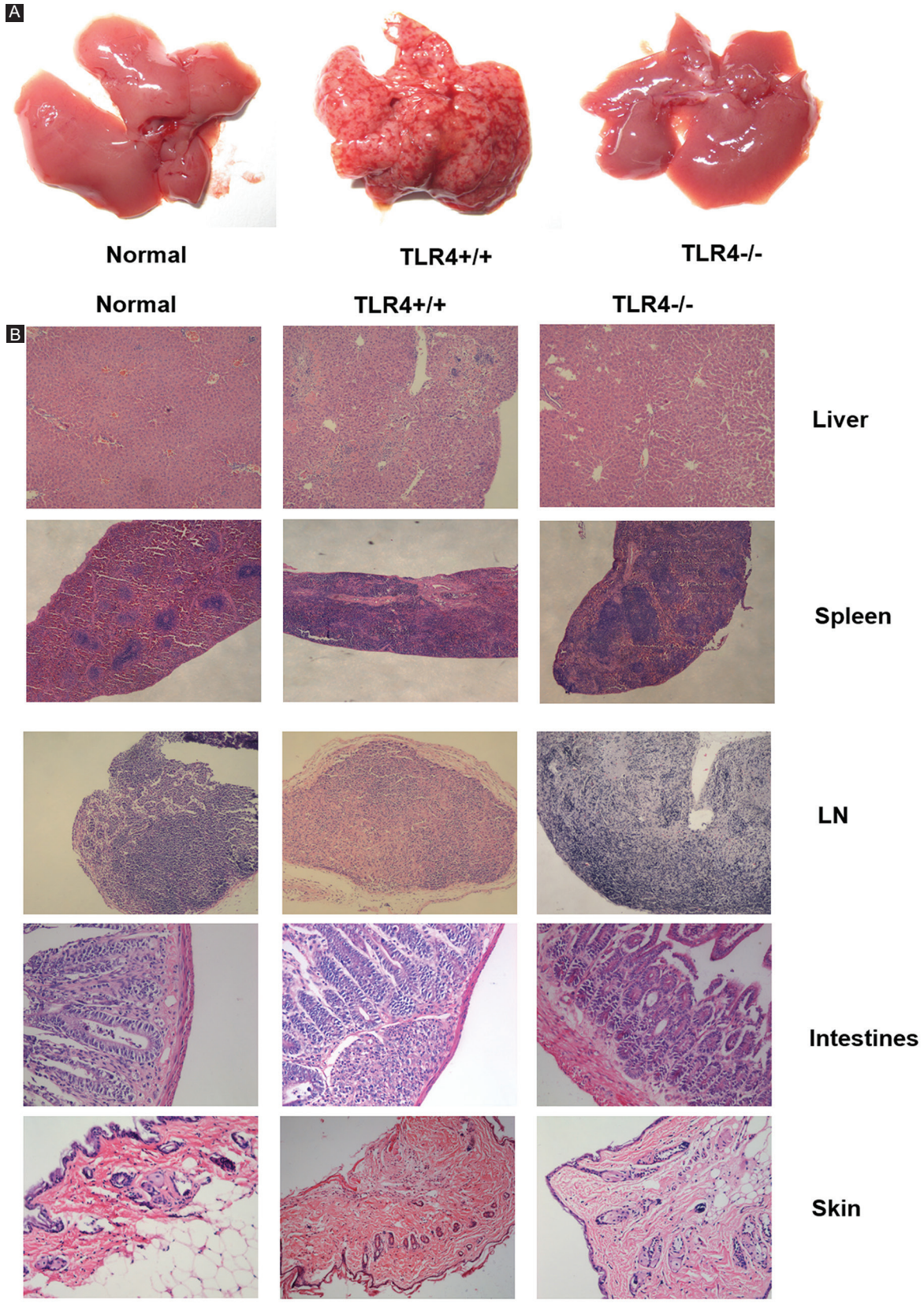

Figure 7. *Histopathological changes indicative of graft-versus-host disease (GVHD) in recipient mice.* **A:** *discrete petechiae were observed on all the liver surfaces of TLR4$^{+/+}$ mice, while no obvious petechiae were observed in TLR4$^{-/-}$ mice.* **B:** *histopathological manifestations of GVHD occurred in organs after allogenic bone marrow transplantation (Normal, TLR4$^{+/+}$ recipient mice and TLR4$^{-/-}$ recipient mice (Liver50×, Spleen50×, LN50×, Intestines ×200, Skin ×100).*

the peripheral blood fraction was fewer, and the mature T lymphocyte proportion in the bone marrow was < 2%, so GVHD caused by simple BMT was less severe or did not occur. However, the levels of lymphocytes in the spleen were elevated. Therefore, the GVHD mouse model should be established by lethal TBI followed by injection of both donor bone marrow cells and splenocytes[21-23]. Researchers have also found that a simple increase in the amount of donor bone marrow cannot improve the implantation rate, but injection of a bone marrow cell and splenocyte suspension with 35% T lymphocytes derived from donor mice into recipient mice can improve the level of implantation[24]. Reports have stated that T-cell numbers between 1×10^6 and 1×10^7 can induce typical GVHD at different times[25]. Bone marrow cell numbers must be higher than 1×10^5 to ensure successful implantation, but it would be better to set the bone marrow cell number above 1×10^7 for hematopoietic reconstitution[26,27]. In our experiment, mice received approximately 1×10^7 bone marrow cells and 2×10^7 splenocytes through the tail vein, which resulted in successful hematopoietic reconstitution and induced GVHD.

Some monitoring indices were used to evaluate recipient mice in our study. Survival curves reflected that compared to C57BL/6 mice, $TLR4^{-/-}$ mice died earlier after irradiation. The mortality of the $TLR4^{-/-}$ mice was highest at 7 days after irradiation. However, if the $TLR4^{-/-}$ mice remained alive, they had a long life span (26.7% lived beyond 65 days) with little graft rejection compared to $TLR4^{+/+}$ mice (13.3% lived beyond 65 days). However, the phenomenon that there was a continual decline in survival through approximately day 30 which was seen in both the $TLR4^{+/+}$ and $TLR4^{-/-}$ cohorts needed further investigate. The WBC count and weight of recipient mice after transplantation were significantly decreased but began increasing as time passed. If GVHD occurs during this time period, the WBC count and weight will fluctuate. The index of those mice that had mild GVHD and a long life span could recover to the level observed before transplantation. We found reduced aGVHD severity in the $TLR4^{-/-}$ mice, but some mice still showed typical signs of GVHD, such as increased eye secretion, ankyloblepharon, lower limb asthenia, and paralysis. Interestingly, some mice exhibited a change in fur color, developing fur the same color as that of the donor mice. These phenomena are similar to clinical GVHD symptoms and signs including dry eye, myalgia, asthenia, and change in fur characteristics[28]. These findings clearly demonstrated that the mouse model of allogeneic BMT is an ideal tool to explore the pathogenesis of GVHD[10].

Were the hematopoietic cells of recipient mice completely cleared after myeloablative radiation? When and how did the mice undergo hematopoietic reconstitution? Previous studies have used only approximate routine peripheral blood tests to judge the time. To understand when $TLR4^{-/-}$ mice show hematopoietic reconstitution and chimerism after transplantation in detail, we monitored the ratio of cells of donor and recipient origin, using anti-H-$2K^b$ and anti-H-$2K^d$ antibodies, by FCM to distinguish the different cell origins so as to detect the chimeric process. The rates of hematopoietic recovery are related to the radiation dose and the input amount of mouse bone marrow cells[29-32]. In general, the lower the radiation dose and the larger the amount of bone marrow cells are, the better the hematopoietic reconstitution. When the input of donor bone marrow cells was 1×10^7, recipient mouse blood cells returned to the beginning level approximately 2 weeks after transplantation in this study. This finding can also provide some reference for clinical work.

Donor T-cell activation by APCs is the most important stage among the three stages described for GVHD[33]. Understanding how host APCs involved in direct delivery are changed into donor APCs also plays an important role in indirect delivery[34]. Therefore, mastering the percentages and sources of APCs and T-cells is very important. We observed these kinds of cells through FCM. Most of the APCs and T-cells in the host mouse spleen were derived from donor cells, and $CD4^+$ T-cells, including memory T-cells, were in the majority in host mice. Furthermore, the ratio of APCs derived from donor mice and the proportion of $CD4^+$ T-cells in the T-cell subsets of $TLR4^{-/-}$ mice were lower than that of $TLR4^{+/+}$ mice. Although APCs in the recipient mouse spleen were predominantly derived from donor cells at 30 days after BMT, other cells, such as epithelial and Langerhans cells, also take on substantial roles as APCs after irradiation. Therefore, the effect that host APCs have by indirectly presenting antigens to donor T-cells cannot be ignored. We also focused on the activation of donor T-cells and the distributions of T-cell subsets in the spleen and found that the proportion of $CD4^+$ T-cells was 1.5 times higher than that of $CD8^+$ T-cells in $TLR4^{+/+}$ mice while the ratio is < 1.5 times in $TLR4^{-/-}$ mice. Histopathological sections revealed that $CD4^+$ and $CD8^+$ T-cells were the main infiltrating

lymphocyte populations and that the amount of $CD4^+$ T-cells was higher than that of $CD8^+$ T-cells in liver tissue with GVHD. The above results showed that $CD4^+$ T-cells played an important role in GVHD, and we, further, investigated the molecular mechanism by which $CD4^+$ T-cells damage the liver in the follow-up study. In addition, we concluded that the proportion of naive T-cells ($CD44^- CD62L^+$) decreased in recipient mice after transplantation, while the proportion of memory T-cells ($CD44^+ CD62L^-$) increased. That is, naive T-cells can transform into memory T-cells through transplantation. A recent study noted that specific activation of memory T-cells from cancer patients can result in the recognition and rejection of transplanted autologous tumor cells. Memory T-cells can be activated by their own tumor antigens in the bone marrow to further recognize antigens presented by dendritic cells and produce a great quantity of apoptotic cells through an immune response[35]. Thus, the increase in memory T-cell frequency after allogeneic transplantation contributes to the immune response against malignant blood tumor cells and may be one mechanism of GVHD.

Conclusion

We established a mouse model of GVHD in $TLR4^{-/-}$ mice and evaluated the model in regard to hematopoietic reconstitution, survival and body weight changes, chimerism, and GVHD severity. The establishment of this platform laid the foundation for further study of the role of the TLR4 gene in the pathogenesis of GVHD and related mechanisms. In addition, the chimerism of the model reflects the cellular mechanisms of GVHD observed clinically and provides new ideas for clinical GVHD treatment strategies.

Funding

This study was supported by the National Natural Science Foundation of China (Project No. 81700201, No. 81770217, No.82100213), Medical and Health Science and Technology Project of Zhejiang Province (Project No. 2014KYB102 and No. 2021KY143) and Natural Science Foundation of Zhejiang Province,China (Grant No.LY22H080004).

Conflicts of interest

The authors declare that they have no conflicts of interest.

Ethical disclosures

Protection of human and animal subjects. The authors declare that the procedures followed were in accordance with the regulations of the relevant clinical research ethics committee and with those of the Code of Ethics of the World Medical Association (Declaration of Helsinki).

Confidentiality of data. The authors declare that no patient data appear in this article.

Right to privacy and informed consent. The authors declare that no patient data appear in this article.

References

1. Ghimire S, Weber D, Mavin E, Wang XN, Dickinson AM, Holler E. Pathophysiology of GvHD and other HSCT-related major complications. Front Immunol. 2017;8:79.
2. Ferrara JL, Chaudhry MS. GVHD: biology matters. Hematology Am Soc Hematol Educ Program. 2018;2018:221-7.
3. Zeiser R, Blazar BR. Acute graft-versus-host disease-biologic process, prevention, and therapy. N Engl J Med. 2017;377:2167-79.
4. Hill L, Alousi A, Kebriaei P, Mehta R, Rezvani K, Shpall E. New and emerging therapies for acute and chronic graft versus host disease. Ther Adv Hematol. 2018;9:21-46.
5. Penack O, Holler E, van den Brink MR. Graft-versus-host disease: regulation by microbe-associated molecules and innate immune receptors. Blood. 2010;115:1865-72.
6. Lorenz E, Schwartz DA, Martin PJ, Gooley T, Lin MT, Chien JW, et al. Association of TLR4 mutations and the risk for acute GVHD after HLA-matched-sibling hematopoietic stem cell transplantation. Biol Blood Marrow Transplant. 2001;7:384-7.
7. Brennan TV, Lin L, Huang X, Cardona DM, Li Z, Dredge K, et al. Heparan sulfate, an endogenous TLR4 agonist, promotes acute GVHD after allogeneic stem cell transplantation. Blood. 2012;120:2899-908.
8. Boieri M, Shah P, Dressel R, Inngjerdingen M. The Role of animal models in the study of hematopoietic stem cell transplantation and GvHD: a historical overview. Front Immunol. 2016;7:333.
9. Zhao Y, Liu Q, Yang L, He D, Wang L, Tian J, et al. TLR4 inactivation protects from graft-versus-host disease after allogeneic hematopoietic stem cell transplantation. Cell Mol Immunol. 2013;10:165-75.
10. Jazbec K, Jež M, Smrekar B, Miceska S, Rožman JŽ, Švajger U, et al. Chimerism and gene therapy-lessons learned from non-conditioned murine bone marrow transplantation models. Eur J Haematol. 2018;100:372-82.
11. Baron F, Sandmaier BM. Chimerism and outcomes after allogeneic hematopoietic cell transplantation following nonmyeloablative conditioning. Leukemia. 2006;20:1690-700.
12. Jaksch M, Uzunel M, Remberger M, Sundberg B, Mattsson J. Molecular monitoring of T-cell chimerism early after allogeneic stem cell transplantation may predict the occurrence of acute GVHD grades II-IV. Clin Transplant. 2005;19:346-9.
13. Hoshino K, Takeuchi O, Kawai T, Sanjo H, Ogawa T, Takeda Y, et al. Cutting edge: toll-like receptor 4 (TLR4)-deficient mice are hyporesponsive to lipopolysaccharide: evidence for TLR4 as the Lps gene product. J Immunol. 1999;162:3749-52.
14. Hill GR, Ferrara JL. The primacy of the gastrointestinal tract as a target organ of acute graft-versus-host disease: rationale for the use of cytokine shields in allogeneic bone marrow transplantation. Blood. 2000;95:2754-9.
15. Nikolic B, Lee S, Bronson RT, Grusby MJ, Sykes M. Th1 and Th2 mediate acute graft-versus-host disease, each with distinct end-organ targets. J Clin Invest. 2000;105:1289-98.
16. Calcaterra C, Sfondrini L, Rossini A, Sommariva M, Rumio C, Ménard S, et al. Critical role of TLR9 in acute graft-versus-host disease. J Immunol. 2008;181:6132-9.
17. Wardill HR, Tissing WJ, Kissow H, Stringer AM. Animal models of mucositis: critical tools for advancing pathobiological understanding and identifying therapeutic targets. Curr Opin Support Palliat Care. 2019;13:119-33.
18. Ghita M, Dunne V, Hanna GG, Prise KM, Williams JP, Butterworth KT. Preclinical models of radiation-induced lung damage: challenges and opportunities for small animal radiotherapy. Br J Radiol. 2019;92:20180473.

19. Cooke KR, Kobzik L, Martin TR, Brewer J, Delmonte J Jr, Crawford JM, et al. An experimental model of idiopathic pneumonia syndrome after bone marrow transplantation: I. The roles of minor H antigens and endotoxin. Blood 1996;88:3230-9.
20. Yañez R, Lamana ML, García-Castro J, Colmenero I, Ramírez M, Bueren JA. Adipose tissue-derived mesenchymal stem cells have *in vivo* immunosuppressive properties applicable for the control of the graft-versus-host disease. Stem Cells. 2006;24:2582-91.
21. Speiser DE, Bachmann MF, Shahinian A, Mak TW, Ohashi PS. Acute graft-versus-host disease without costimulation via CD28. Transplantation. 1997;63:1042-4.
22. Dang N, Lin Y, Rutgeerts O, Sagaert X, Billiau AD, Waer M, et al. Solid tumor-induced immune regulation alters the GvHD/GvT paradigm after allogenic bone marrow transplantation. Cancer Res. 2019;79:2709-21.
23. Hashimoto N, Narumi S, Itabashi Y, Hakamada K, Sasaki M. Efficacy of donor splenocytes mixed with bone marrow cells for induction of tolerance in sublethally irradiated mice. Transpl Immunol. 2002;10:37-41.
24. Kuwatani M, Ikarashi Y, Mineishi S, Asaka M, Wakasugi H. An irradiation-free nonmyeloablative bone marrow transplantation model: importance of the balance between donor T-cell number and the intensity of conditioning. Transplantation. 2005;80:1145-52.
25. Contassot E, Murphy W, Angonin R, Pavy JJ, Bittencourt MC, Robinet E, et al. *In vivo* alloreactive potential of *ex vivo*-expanded primary T lymphocytes. Transplantation 1998;65:1365-70.
26. Lemoli RM, Bertolini F, Petrucci MT, Gregorj C, Ricciardi MR, Fogli M, et al. Functional and kinetic characterization of granulocyte colony-stimulating factor-primed CD34- human stem cells. Br J Haematol. 2003;123:720-9.
27. Bolaños-Meade J, Vogelsang GB. Novel strategies for steroid-refractory acute graft-versus-host disease. Curr Opin Hematol. 2005;12:40-4.
28. Spitzer TR. Engraftment syndrome following hematopoietic stem cell transplantation. Bone Marrow Transplant. 2001;27:893-8.
29. Pecora AL. Impact of stem cell dose on hematopoietic recovery in autologous blood stem cell recipients. Bone Marrow Transplant. 1999;23 Suppl 2:S7-12.
30. van Os R, Thames HD, Konings AW, Down JD. Radiation dose-fractionation and dose-rate relationships for long-term repopulating hemopoietic stem cells in a murine bone marrow transplant model. Radiat Res. 1993;136:118-25.
31. Desai A, Zhang Y, Park Y, Dawson DM, Larusch GA, Kasturi L, et al. A second-generation 15-PGDH inhibitor promotes bone marrow transplant recovery independently of age, transplant dose and granulocyte colony-stimulating factor support. Haematologica. 2018;103:1054-64.
32. Chang J, Feng W, Wang Y, Allen AR, Turner J, Stewart B, et al. (28)Si total body irradiation injures bone marrow hematopoietic stem cells via induction of cellular apoptosis. Life Sci Space Res (Amst). 2017;13:39-44.
33. Kataoka Y, Iwasaki T, Kuroiwa T, Seto Y, Iwata N, Hashimoto N, et al. The role of donor T cells for target organ injuries in acute and chronic graft-versus-host disease. Immunology. 2001;103:310-8.
34. Paczesny S, Hanauer D, Sun Y, Reddy P. New perspectives on the biology of acute GVHD. Bone Marrow Transplant. 2010;45:1-11.
35. Beckhove P, Feuerer M, Dolenc M, Schuetz F, Choi C, Sommerfeldt N, et al. Specifically activated memory T cell subsets from cancer patients recognize and reject xenotransplanted autologous tumors. J Clin Invest. 2004;114:67-76.